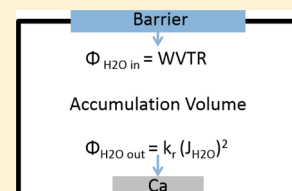


Oxidation Kinetics of Calcium Films by Water Vapor and Their Effect on Water Vapor Transmission Rate Measurements

Daniel J. Higgs,[†] Matthias J. Young,[‡] Jacob A. Bertrand,[†] and Steven M. George^{*,†,§}[†]Department of Chemistry and Biochemistry, [‡]Department of Chemical and Biological Engineering, and [§]Department of Mechanical Engineering, University of Colorado, 215 UCB, Boulder, Colorado 80309-0215, United States

ABSTRACT: The oxidation of calcium films by water vapor is the basis of the “Ca test” used to measure low water vapor transmission rates (WVTRs) through gas diffusion barriers. The Ca test assumes that the Ca film oxidation rate is linear with H₂O flux transmitted through the barrier. However, lag times are often observed during WVTR measurements that could indicate that the Ca film oxidation rate is not linear with H₂O flux. To explore the oxidation kinetics of Ca films by H₂O vapor, a new Ca test was developed based on quartz crystal microbalance (QCM) measurements. The QCM measures the mass gain that occurs as the Ca film oxidizes according to the reaction: $\text{Ca} + 2\text{H}_2\text{O} \rightarrow \text{Ca}(\text{OH})_2 + \text{H}_2$. The QCM measurements observed a long lag time before the Ca films began to oxidize. The Ca film oxidation was studied using a number of experimental configurations. In all cases, the Ca film oxidation was not linear with H₂O flux to the Ca film. These results suggest that the nonlinearity of Ca film oxidation in many WVTR experiments may result from the nonlinear oxidation of the Ca film itself. Additional measurements of the times required for complete Ca film oxidation versus H₂O flux at constant temperatures were consistent with oxidation kinetics that were second-order in H₂O flux. The nonlinear Ca film oxidation raises doubts about the validity of WVTR measurements using the Ca test. However, modeling based on the measured nonlinear Ca film oxidation kinetics suggests that the Ca test can yield reliable WVTR measurements under special circumstances. These circumstances occur when the accumulation volume between the barrier and the Ca film is small enough to allow for steady state pressure conditions where the H₂O flux transmitted through the barrier is equivalent to the H₂O flux removed by oxidation of the Ca film. The lag time is associated with the time required to obtain the steady state pressure in the accumulation volume.



I. INTRODUCTION

Calcium is a metal that is easily oxidized by H₂O vapor.^{1–3} This oxidation converts metallic and electrically conducting calcium to more transparent and insulating calcium hydroxide, Ca(OH)₂.^{3,4} This transition is the basis of the “Ca test” used to measure H₂O transport through materials such as gas diffusion barrier films.⁵ Ultralow water vapor transmission rates (WVTRs) of <10^{−6} g/(m²day) are required for organic electronic devices to reach device lifetimes of >10000 h.⁶ These requirements arise from the sensitivity of the low work function metals (e.g., Ca, Li, Mg) in these devices to water oxidation. The Ca test has been one of the main techniques utilized to measure these ultralow WVTRs.

During application of the Ca test, a gas diffusion barrier separates a Ca metal film from H₂O vapor at a controlled humidity. The water that is transported through the gas diffusion barrier oxidizes the Ca metal by the reaction: $\text{Ca} + 2\text{H}_2\text{O} \rightarrow \text{Ca}(\text{OH})_2 + \text{H}_2$.^{3,4} The optical transmittance,^{5,7,8} electrical conductance,^{9–11} or size of the oxidized areas^{12,13} of the Ca film are then monitored during the Ca test as the reflective and electrically conducting Ca film oxidizes to the transparent and electrically insulating calcium hydroxide film. The rate of change in the optical transmission, electrical conductance or oxidation area is used to calculate the WVTR.

The Ca test methods rely on the assumption that the calcium oxidation is linear with the H₂O exposure. This assumption can be traced back to the “Pilling and Bedworth Ratio”, which is the ratio of the volume of the metal oxide to the volume of the

corresponding metal.¹⁴ If this ratio is less than unity, then the metal oxide should be porous and allow the oxidant to continuously oxidize the metal.¹⁴ Consequently, the optical transmission and electrical conductance of the Ca films should change linearly with water exposure. However, there have been only a few previous studies of Ca oxidation kinetics.^{1–3} These studies reveal complicated oxidation kinetics that do not support the assumption of linear calcium oxidation.^{1–3}

One early study of calcium oxidation by H₂O revealed logarithmic kinetics and a negative activation energy.³ Another study found calcium oxidation by water “surprisingly complex” and could not fit the results with any functional form.¹ A third study concluded that calcium oxidation by H₂O may be linear below 150 °C and logarithmic at 300 °C, with no single oxidation mechanism observable above 150 °C.² This same study also measured a decrease in oxidation rate with increasing temperature.²

Our own previous work has focused on Ca film oxidation using the electrical Ca test.^{15,16} These studies showed that there was a very nonlinear decrease in calcium conductance with water exposure at 70 °C.¹⁶ Additionally, results from combined optical and electrical tests on Al₂O₃ barriers grown directly on Ca films showed that when the calcium conductance reached its

Special Issue: John C. Hemminger Festschrift

Received: June 4, 2014

Revised: August 12, 2014

Published: August 13, 2014



final value, there were unreacted, metallic calcium “islands” that were electrically insulated from the electrodes.¹⁵ Other studies have confirmed the nonhomogeneous oxidation of calcium with real-time atomic force microscope (AFM) measurements. These results show the formation of “columns” of the calcium hydroxide product.^{17,18} These various observations suggest that calcium does not oxidize uniformly.

The oxidation of calcium by dry oxygen is much slower than the oxidation of calcium by H_2O .⁴ Significant oxidation of calcium by O_2 is not observed until much higher temperatures of $>400^\circ\text{C}$.^{19–21} At these higher temperatures, the oxidation kinetics are also very complex.^{19–21} The initial oxidation of calcium by O_2 follows parabolic kinetics.^{19,21} The latter stages of calcium oxidation can be linear.^{19,21} However, the overall oxidation kinetics are very complicated and do not follow any simple interpretation.

We have developed a mass-based Ca test to avoid the complications of interpreting the electrical conductance during nonuniform calcium oxidation. A quartz crystal microbalance (QCM) was coated with Ca metal and employed as the water sensor in place of a 4-wire conductance measurement.¹⁶ QCMs measure the frequency change of a piezoelectric quartz crystal oscillating at its resonance frequency. As mass is deposited on the crystal, the frequency shifts. This change in frequency is proportional to the mass gain on the crystal. The QCM has sensitivity to mass changes as small as $\sim 0.2\text{ ng/cm}^2$. This sensitivity allows small mass changes during H_2O oxidation to be measured to determine calcium oxidation kinetics.

The oxidation kinetics of Ca films by water vapor were measured by coating the QCM crystal with Ca thin films with thicknesses of 100–1000 nm. Oxidation kinetics were measured for several experimental configurations at a variety of temperatures and H_2O fluxes. Diffusion models were also used to determine the predicted results if the important assumptions of the Ca test are valid. The diffusion models disagree with the measurements and reveal the pronounced nonlinear oxidation kinetics of the Ca films. However, the modeling does suggest that reliable WVTR values can be obtained under specific conditions.

II. EXPERIMENTAL SECTION

A. QCM Measurements. All experiments reported in this paper used chromium-plated QCM crystals. Our early work first used gold-coated QCM crystals that were then covered with thermally evaporated calcium metal. Gold–calcium alloying was observed at around 60°C and led to a nonreproducible mass gain response. For all experiments, QCM quartz crystals (6 MHz, Inficon pattern, Cr-plated, Colorado Crystal Corp.) were assembled in a custom-made aluminum holder under the inert atmosphere of a N_2 glovebox.¹⁵ A custom aluminum mask was secured on the crystals to expose a 0.316 cm^2 circular area of the crystal to subsequent Ca deposition. The holder/crystal/mask assembly was transferred from the glovebox to a physical vapor deposition (PVD) chamber using a transfer arm.¹⁵ The Ca films were deposited using thermal evaporation. Using an in situ QCM to determine the calcium thickness, the QCM crystals were coated with Ca films with thicknesses of 100 nm, 275 or 1000 nm for different experiments. These various Ca film thicknesses provided adequate time for reliable data acquisition.

After thermal evaporation of calcium onto the QCM crystals, the holder/crystal/mask assembly was returned to the glovebox via the transfer arm. The crystal was removed from the holder and mask and inserted into a QCM cool drawer sensor head

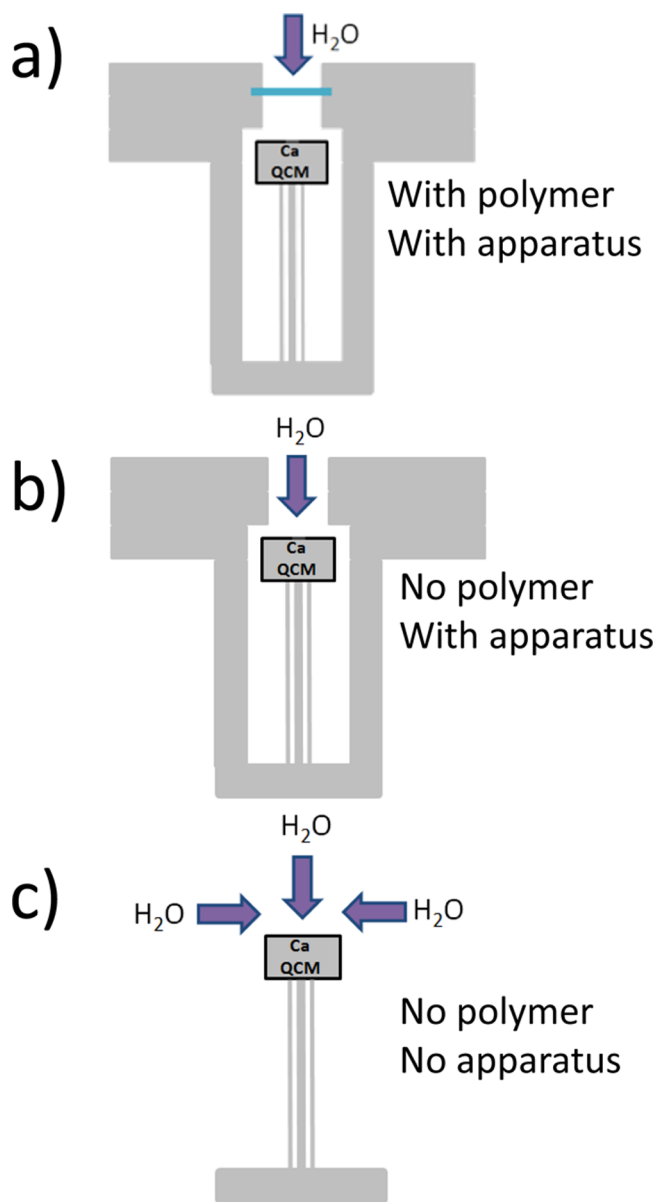


Figure 1. Three experimental configurations that investigated Ca film oxidation by H_2O vapor: (a) “with polymer, with apparatus”; (b) “no polymer, with apparatus”; and (c) “no polymer, no apparatus”.

(Maxtek) on a Conflat flange. The sensor head was then assembled into the appropriate measurement apparatus under inert N_2 atmosphere in the glovebox. Figure 1 shows the three experimental configurations that investigated the oxidation of Ca films under various conditions.

Figure 1a shows the “with polymer, with apparatus” configuration where a bare PEN polymer sample is positioned between the H_2O vapor conditions and the Ca film. For a mass increase to be observed by the QCM, water must transmit through the bare PEN polymer, enter the chamber, then react with the calcium on the QCM crystal. The PEN polymer was mounted as previously reported.¹⁶ Flanges were sealed with Conflat gaskets or Viton O-rings. An O-ring-sealed plug was also placed above the PEN polymer in the opening of the apparatus during assembly. This plug was then removed after the apparatus was at the stable desired temperature in the humidity chamber.

Figure 1b shows the “no polymer, with apparatus” configuration. This setup was used to measure the oxidation of calcium without the PEN polymer sample. For a mass increase to be observed by the QCM in this setup, water only needs to diffuse through the opening in the apparatus and the open volume of the chamber before reacting with the calcium on the QCM crystal. An O-ring-sealed plug was placed in the opening of the apparatus during assembly in the glovebox. This plug was then removed after the apparatus was at the stable desired temperature in the humidity chamber.

Figure 1c shows a schematic of the “no polymer, no apparatus” setup. This setup was used to measure the oxidation of calcium without bare PEN polymer samples and without any enclosure. The QCM crystal is completely open to the water flux in this configuration. However, a new sealing system was required to initiate experiments using this apparatus. This sealing system was assembled over the QCM in the glovebox. The seal was then removed after the apparatus was at the stable desired temperature in the humidity chamber.

The sealing system was comprised of an aluminum collar and an aluminum cap. The Conflat flange on the aluminum collar was connected to the Conflat flange on the QCM using a copper gasket. The aluminum cap was sealed to the aluminum collar with a Viton O-ring seal under the inert atmosphere of the glovebox. Because experiments at high temperatures and high humidities only lasted on the order of seconds to minutes, a device was created to allow removal of the aluminum cap without opening the door to the humidity chamber. A linear actuator cable was attached to a fork that held the aluminum cap. When the linear actuator was pulled outside the humidity chamber, the aluminum cap was pulled away from the aluminum collar by overcoming the friction of the Viton O-ring seal, and the QCM was exposed to the desired humidity.

The various experimental configurations shown in Figure 1 were placed inside an ESPEC humidity chamber with controlled temperature and relative humidity.¹⁶ Conditions were varied for different experiments. Temperature varied from 30 to 85 °C and %RH varied from 15 to 87%. The QCM was connected via a BNC cable to an Inficon Q-pod. Q-pod software was used to record the frequency and mass gain data that was saved as a .txt file and later processed using Igor and Excel software.

Calcium oxidation is very slow at low water fluxes, $J_{\text{H}_2\text{O}}$, and experiments may require months to fully oxidize Ca films with thicknesses of 100 or 275 nm. Consequently, most experiments were performed at high water fluxes. These water fluxes to the Ca film are much higher than would exist during a Ca test for a gas diffusion barrier with a low WVTR. Experiments at H_2O vapor pressures of 7×10^{-5} Torr and 1×10^{-7} Torr were also performed to explore the effect of low water fluxes on calcium oxidation.

The experiments at low H_2O vapor pressures of 7×10^{-5} Torr and 1×10^{-7} Torr required the use of a small high vacuum chamber. This vacuum chamber was positioned inside the temperature controlled oven of the ESPEC humidity chamber. This vacuum chamber enclosed the QCM and also contained an ionization gauge to measure the H_2O pressure. This vacuum chamber was pumped with a turbomolecular pump (Pfeiffer Balzers TPU 050) backed by a mechanical pump. H_2O was constantly leaked into the QCM chamber through a high vacuum precision leak valve. The water input was regularly adjusted to maintain the target H_2O pressure.

B. Diffusion Model. The diffusion of water through the test apparatus was modeled using the one-dimensional form of Fick's second law:²²

$$\frac{\partial C_w[t, z]}{\partial t} = D_{\text{aw}} \frac{\partial^2 C_w[t, z]}{\partial z^2} \quad (1)$$

Equation 1 was solved using the following boundary and initial conditions:

$$C_w[t > 0, 0] = C_0 \quad (2)$$

$$C_w[t > 0, h] = 0 \quad (3)$$

$$C_w[0, z] = 0 \quad (4)$$

In these equations, C_w is the H_2O concentration, D_{aw} is the diffusivity of H_2O in air, and h is the distance from the opening of the Ca test apparatus to the Ca film surface. The boundary condition in eq 3 assumes the instantaneous diffusion of H_2O through calcium hydroxide and the reaction of every H_2O molecule that reaches the calcium surface. Additionally, there were no temperature gradients in the test apparatus and no radial dependence on H_2O concentration.

With these assumptions and boundary conditions, the solution to eq 1 takes the form of a Fourier series:²³

$$C_w[t, z] = C_w^{\text{ss}} + \sum_{n=1}^{\infty} A_n e^{-\lambda_n^2 D_{\text{aw}} t} \sin[\lambda_n z] \quad (5)$$

where

$$\lambda_n = \frac{n\pi}{h} \quad (6)$$

$$A_n = \int_0^h \frac{2}{h} (C_w[0, z] - C_w^{\text{ss}}) \sin[\lambda_n z] dz \quad (7)$$

$$C_w^{\text{ss}} = C_0 \left(1 - \frac{z}{h} \right) \quad (8)$$

The flux of H_2O onto the Ca film surface can then be calculated as

$$J_h[t] = -D_{\text{aw}} \frac{\partial C_w[t, z]}{\partial z} \Big|_{z=h} \quad (9)$$

The total moles of H_2O that react with the Ca film surface, N , can be expressed as

$$N[t] = \int_0^t f[t'] dt' \quad (10)$$

In eq 10, f is equal to J_h under the assumption that every H_2O molecule reacts upon collision with the Ca film surface. Simulations using this model include only the first 20 terms of the Fourier series given in eq 5.

III. RESULTS AND DISCUSSION

A. Polymer with Apparatus. The QCM-based Ca test was used to examine water transmission through a bare heat-stabilized polyethylene-naphthalate polymer (200 μm , Teonex HSPEN, Teijin Dupont Films) using the configuration shown in Figure 1a at 30 °C and 20% RH (6.4 Torr H_2O). PEN is reported to have a WVTR of ~ 1.2 g/(m^2 day) for a thickness of 125 μm .²⁴ Figure 2 shows the mass gain versus time for a 100 nm Ca film on the QCM crystal. The solid line results from the overlap of multiple data points. These results reveal that

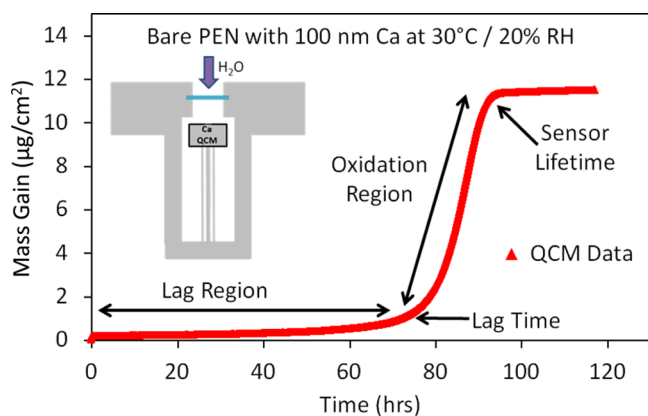


Figure 2. Mass gain vs time for bare PEN polymer mounted in the test apparatus as shown in Figure 1a with 100 nm Ca film on QCM at 30 °C and 20% RH. Mass gain vs time curve is used to define lag region, lag time, oxidation region, and sensor lifetime.

there is a long lag time and the Ca film oxidation is not linear. Similar results were earlier observed for Ca film oxidation using the electrical conductance Ca test.¹⁶

The general shape of the curve in Figure 2 can be separated into regions. First, an initial period of very slow mass increase is observed between $t = 0$ and $t \sim 75$ h. This section is termed the “lag region”. The next section where the mass increases rapidly and then reaches a constant rate is termed the “oxidation region”. This section occurs from $t \sim 75$ h to $t \sim 95$ h. The “lag time” is defined as the time from $t = 0$ to the beginning of the “oxidation region”. The “sensor lifetime” is defined as the time from $t = 0$ to the end of the “oxidation region”. The “final mass gain” is defined as the mass at the end of the “oxidation region”.

A final mass gain of $12 \mu\text{g}/\text{cm}^2$ is observed in Figure 2. The sensor lifetime for this experiment with a PEN polymer is 90 h. The measured mass gain of $12 \mu\text{g}/\text{cm}^2$ is consistent with the predicted mass gain of $13.1 \mu\text{g}/\text{cm}^2$ that would be expected if a 100 nm film of calcium fully reacted to form $\text{Ca}(\text{OH})_2$ according to the reaction: $\text{Ca} + 2\text{H}_2\text{O} \rightarrow \text{Ca}(\text{OH})_2 + \text{H}_2$. The mass of a 100 nm Ca film is $15.6 \mu\text{g}/\text{cm}^2$. The mass of the 100 nm Ca film completely oxidized to $\text{Ca}(\text{OH})_2$ is $28.7 \mu\text{g}/\text{cm}^2$.

Three different WVTRs can be calculated from the data shown in Figure 2. The WVTR calculated from the lag region is $4.2 \times 10^{-4} \text{ g}/(\text{m}^2 \text{ day})$. The WVTR calculated from the oxidation region is $1.4 \times 10^{-2} \text{ g}/(\text{m}^2 \text{ day})$. Lastly, by dividing the final mass gain by the sensor lifetime, the average WVTR over the entire experiment is $3.4 \times 10^{-3} \text{ g}/(\text{m}^2 \text{ day})$. All three of these WVTRs for the 200 μm PEN film are orders of magnitude lower than the reported WVTR value of $1.2 \text{ g}/(\text{m}^2 \text{ day})$ for a 125 μm PEN film.²⁴

The results in Figure 2 displayed a pronounced nonlinear response in mass gain versus time. In addition, the measured WVTR was much lower than the expected WVTR value of $1.2 \text{ g}/(\text{m}^2 \text{ day})$ for the 125 μm PEN film. These results could be related to H_2O reservoir effects in the PEN film. However, H_2O reservoir effects in PEN have been discounted by earlier studies.¹⁶ These results could also be attributed to other factors including the nonlinear and noninstantaneous oxidation of the Ca film. To understand these results, the PEN film was removed to measure the Ca film oxidation without any complication from the polymer sample.

B. No Polymer with Apparatus. Experiments were performed using the configuration in Figure 1b without a

polymer sample present in the test apparatus. In this configuration, water was free to diffuse from the humidity chamber through the opening in the apparatus. The diameter of the opening in the apparatus was 0.75 in. The calcium-coated QCM crystal was positioned 5 cm below the front face of the apparatus. The H_2O diffusion occurred in air at atmospheric pressure. These experiments were performed at 30 °C, 20%RH (6.4 Torr H_2O) conditions and with a 100 nm Ca film on the QCM crystal.

Figure 3 shows the mass gain of the QCM versus time for a 100 nm Ca film on the QCM crystal. The solid line results from

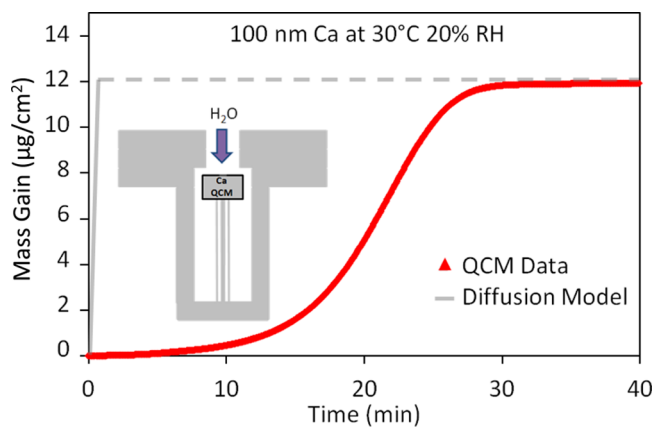


Figure 3. Mass gain vs time for 100 nm Ca film on QCM at 30 °C and 20% RH with no polymer mounted in the test apparatus, as shown in Figure 1b.

the overlapping data points and the gray line is the expected mass gain from diffusion calculations. The expected mass gain assumes instantaneous oxidation when the Ca film is exposed to water. Figure 3 shows a very similar qualitative shape compared with Figure 2. However, the time scale on the horizontal axis is significantly different. The sensor lifetime in Figure 3 with no polymer was ~ 30 min. In comparison, the sensor lifetime was ~ 90 h in Figure 2, with a polymer restricting the H_2O diffusion.

The observation of qualitatively similar lag and oxidation regions with different time scales in Figures 2 and 3 argues that these regions are the result of the Ca film because the polymer is not present in the apparatus yielding the results in Figure 3. The sensor lifetime of ~ 30 min in Figure 3 is also much greater than the predicted lifetime of ~ 1 min determined from diffusion calculations. This discrepancy suggests that the lag region cannot be attributed to diffusion through the apparatus. This discrepancy argues for the nonlinear, noninstantaneous oxidation of the Ca film.

Three different WVTRs can be calculated from the lag region, oxidation region, and mass gain averaged over the sensor lifetime in Figure 3. These WVTRs are $1.6 \times 10^{-1} \text{ g}/(\text{m}^2 \text{ day})$ from the lag region, $1.3 \text{ g}/(\text{m}^2 \text{ day})$ from the oxidation region, and $7.1 \times 10^{-1} \text{ g}/(\text{m}^2 \text{ day})$ from the mass gain averaged over the sensor lifetime. In comparison, an effective WVTR can be calculated based on the H_2O flux that enters the opening of the apparatus. This effective WVTR under atmospheric conditions of 30 °C and 20% RH is $3.2 \times 10^8 \text{ g}/(\text{m}^2 \text{ day})$.

The measured WVTRs are orders of magnitude lower than the effective WVTR of $3.2 \times 10^8 \text{ g}/(\text{m}^2 \text{ day})$. This large discrepancy indicates that the oxidation of the Ca film is not instantaneous. The shape of the mass gain versus time also reveals that the oxidation kinetics are not linear. To understand

these results with no polymer, the effect of the apparatus on measurements was explored by conducting an additional set of experiments without the enclosure around the QCM.

C. No Polymer and No Apparatus. To investigate the role of the apparatus, experiments were performed without the apparatus using the configuration shown in Figure 1c. A standard Maxtek QCM head on a 2.75 in. Conflat flange was used without any surrounding apparatus. These experiments were performed at 30 °C and 20% RH (6.4 Torr H₂O) with a 100 nm Ca film on the QCM crystal. Figure 4 displays results

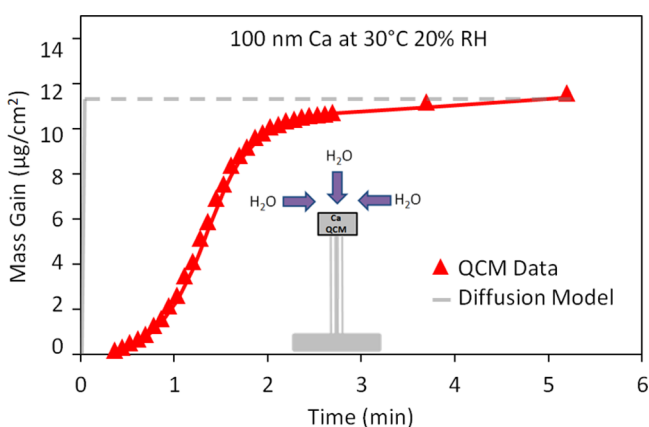


Figure 4. Mass gain vs time for 100 nm Ca film on QCM at 30 °C and 20% RH with no polymer and no test apparatus, as shown in Figure 1c.

from this experiment without the apparatus. The triangular data points are connected with a moving average line to guide the eye. For this experiment, the sensor lifetime is only ~2.5 min.

A comparison between Figures 3 and 4 indicates that the apparatus affects the water flux reaching the QCM. This effect results from the limited solid angle of H₂O flux incident on the Ca film when the apparatus surrounds the QCM using the experimental configuration shown in Figure 1b. The H₂O flux that enters the opening of the apparatus is also diluted by filling the volume of the apparatus. In addition, the difference could be magnified by water absorbing on the interior walls of the apparatus or the diffusion of water being slowed by the outward diffusion of N₂. These additional differences may occur because the apparatus was assembled and sealed under N₂ in a glovebox at a slightly higher pressure than atmospheric pressure.

These experiments without either the apparatus or a polymer sample showed a lag time of ~30 s and a sensor lifetime of ~2.5 min. In comparison, diffusion calculations assuming that the Ca film reacts instantly with H₂O predict the full oxidation of the Ca film in 2.4 s. This time of 2.4 s is the time required for enough H₂O to collide with the Ca surface to react with the entire Ca film assuming a reactive sticking coefficient of unity.

Three different WVTRs can be calculated from the lag region, oxidation region and mass gain averaged over the sensor lifetime in Figure 4. These WVTRs are 2.7 g/(m² day) from the lag region, 1.2×10^1 g/(m² day) from the oxidation region, and 8.2 g/(m² day) from the mass gain averaged over the sensor lifetime. These measured WVTRs are orders of magnitude lower than the effective WVTR of 3.2×10^8 g/(m² day) based on the H₂O flux incident on the Ca film.

The results in Figures 2–4 all suggest that the Ca film does not oxidize instantaneously. There is a significant delay in calcium oxidation at the initial stages of the H₂O exposure. Even when the Ca film oxidizes more rapidly in the oxidation

region, the Ca film does not oxidize as fast as when assuming that the Ca film oxidizes instantaneously. Because these experiments with 100 nm Ca films only lasted ~2.5 min, additional experiments were performed with Ca films with thicknesses of 1000 nm.

D. No Polymer, No Apparatus, 1000 nm Ca. Thicker Ca films of 1000 nm were tested with the configuration shown in Figure 1c to provide even more time for data collection. A set of experiments at 30 °C with 1000 nm thick Ca films investigated the effect of relative humidities of 20, 40, 60, and 80% RH (6.4, 12.7, 19.1, and 25.4 Torr H₂O) on the sensor lifetime. The results are shown in Figure 5. The solid lines

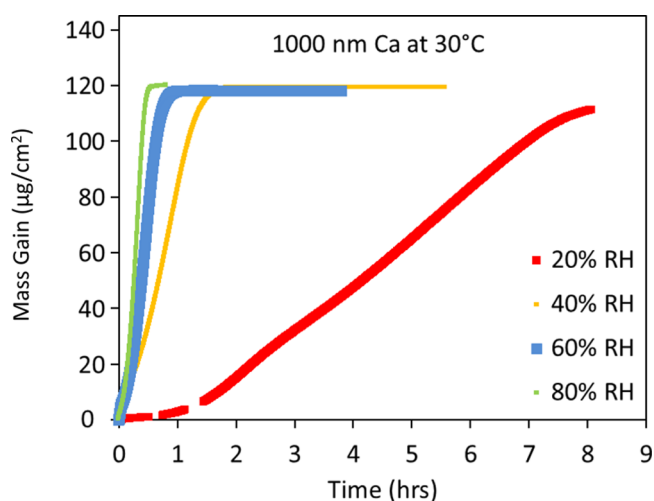


Figure 5. Mass gain vs time for 1000 nm Ca film on QCM at 30 °C and relative humidities of 20%RH, 40%RH, 60%RH, and 80%RH using the experimental configuration shown in Figure 1c.

result from the overlap of multiple data points. The gaps in the line for 20% RH occurred because of two brief computer outages.

Figure 5 shows that the 1000 nm Ca films tested at 20% RH showed an extremely long sensor lifetime of ~8 h. As the relative humidity was doubled from 20% to 40%, the sensor lifetime should reduce by a factor of 2 if the Ca film oxidation kinetics are linear. However, this expectation was not observed. The sensor lifetime for the 1000 nm Ca film at 40% RH was ~1.7 h compared with 8 h for the 20% RH experiment. Further results at 60% RH and 80% RH continue to show this non-linear behavior.

E. Temperature and Water Flux Dependence of Calcium Oxidation Kinetics. Experiments at various temperatures and water fluxes were performed using the configuration in Figure 1c to explore how different temperature and water fluxes affect the Ca film oxidation kinetics. These experiments examined the oxidation of Ca films with a thickness of 275 nm at 30, 50, and 70 °C and at relative humidities of 20 to 80% RH. The Ca film thickness of 275 nm was chosen to compare with previous studies that used similar Ca film thicknesses with the electrical Ca test.¹⁶

The sensor lifetime was determined to be inversely dependent on the square of the water flux, $J_{\text{H}_2\text{O}}$. Figure 6 shows the sensor lifetime at 30, 50, and 70 °C versus $1/(J_{\text{H}_2\text{O}})^2$. The gray lines are the linear best fits to the sensor lifetimes. The linear relationship between the sensor lifetime and $1/(J_{\text{H}_2\text{O}})^2$ is consistent with Ca film oxidation occurring with second-order

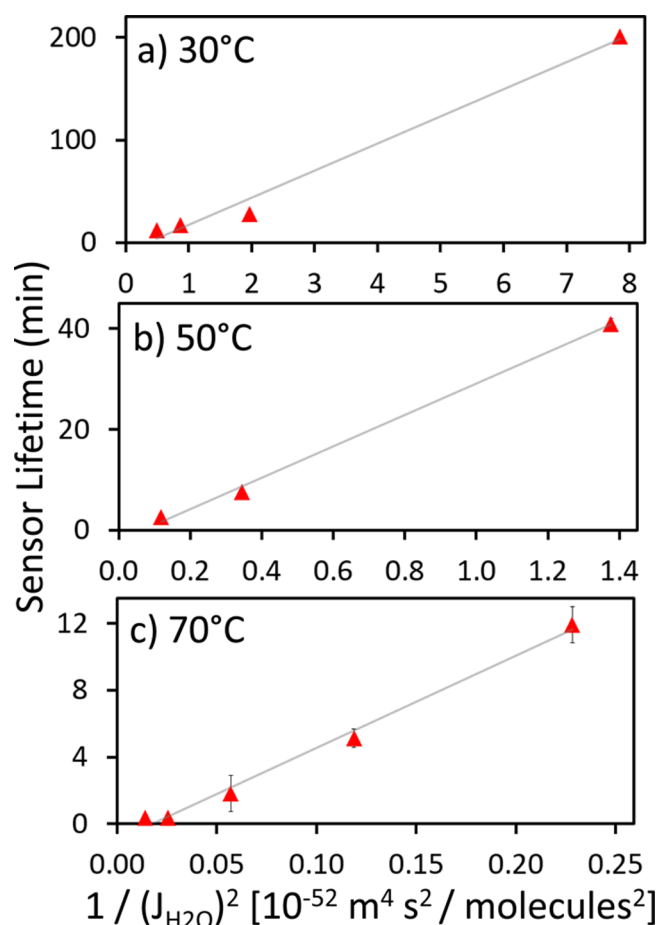


Figure 6. Sensor lifetimes vs $1/(J_{\text{H}_2\text{O}})^2$ for 275 nm Ca film at 30, 50, and 70 °C using the experimental configuration shown in Figure 1c.

kinetics. Second-order kinetics are also consistent with the results in Figure 5 where the sensor lifetime decreased much more than a factor of 2 with the doubling of the water flux. The calcium oxidation kinetics are not linear with the water flux.

The second-order kinetics can be qualitatively explained by the reaction of water with calcium: $\text{Ca} + 2\text{H}_2\text{O} \rightarrow \text{Ca}(\text{OH})_2 + \text{H}_2$. This reaction is understood to be a two-step process according to $\text{Ca} + \text{H}_2\text{O} \rightarrow \text{CaO} + \text{H}_2$ and then $\text{CaO} + \text{H}_2\text{O} \rightarrow \text{Ca}(\text{OH})_2$.¹ This two-step reaction would not necessarily lead to second-order kinetics. However, this two-step reaction process could exhibit second-order kinetic behavior depending on the reaction mechanism and which reaction steps are rate-limiting.

Experiments with fixed $J_{\text{H}_2\text{O}}$ were performed using the configuration in Figure 1c to investigate the effect of temperature on sensor lifetime. The %RH was adjusted to keep $J_{\text{H}_2\text{O}}$ fixed while the temperature was changed for each experiment. Figure 7 shows the sensor lifetime versus temperatures between 45 and 85 °C for Ca films with thicknesses of 275 nm. The water flux was $J_{\text{H}_2\text{O}} = 2.9 \times 10^{26}$ molecules/(m² s). Figure 7 reveals that the sensor lifetime increased with increasing temperature.

The kinetic processes occurring during H₂O oxidation of Ca films involve the adsorption, reaction, and desorption of H₂O, as shown in Figure 8. At fixed $J_{\text{H}_2\text{O}}$, the H₂O adsorption rate will be constant if the H₂O sticking coefficient is constant versus temperature. In contrast, the H₂O desorption rate is expected to increase with temperature. Therefore, a decreasing oxidation

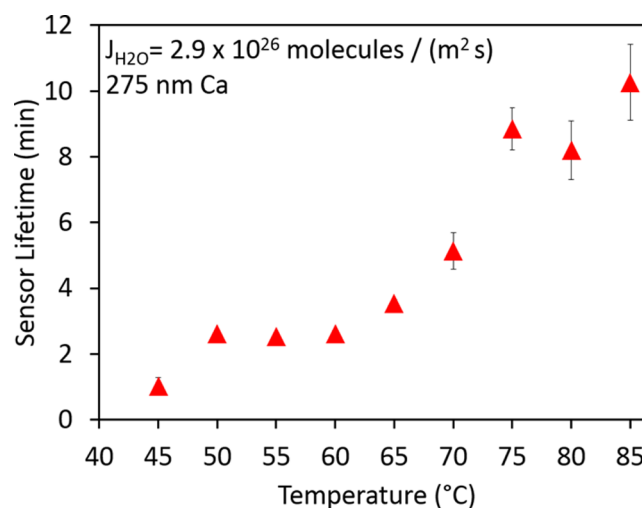


Figure 7. Sensor lifetimes vs temperature for 275 nm Ca film at fixed H₂O flux of $J_{\text{H}_2\text{O}} = 2.9 \times 10^{26}$ molecules/(m² s).

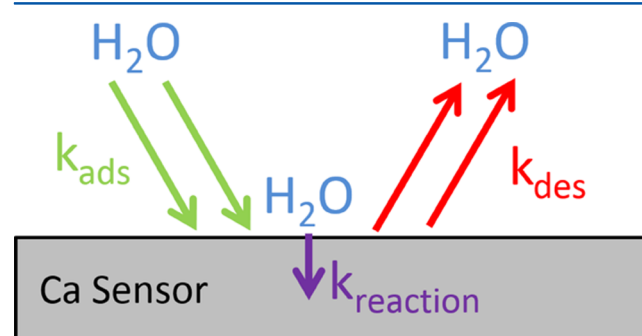


Figure 8. Schematic of H₂O adsorption, desorption, and reaction processes involved during calcium oxidation by H₂O vapor.

rate with increasing temperature could be observed if the increasing H₂O desorption rate leads to a smaller number of H₂O molecules available to react with the Ca film at higher temperatures.

Surface reaction kinetics that decrease at higher surface temperatures are often explained by the “precursor mediated desorption model”.²⁵ The precursor mediated desorption model predicts that the reaction rate will decrease as temperature increases if $E_d > E_r$, where E_d is the activation barrier for desorption and E_r is the activation barrier for reaction. There are many examples of surface reaction kinetics that follow the precursor mediated desorption model. Some examples include the reactive sticking coefficients for N₂ on W(100) surfaces,²⁵ O₂ on Pt(111) surfaces,²⁶ and O₂ and SiH₂Cl₂ on Si(111)7 × 7 surfaces.^{27,28}

The sensor lifetimes in Figure 7 can be graphed in an Arrhenius plot to determine the negative activation barrier that is consistent with the slower oxidation rates at higher temperatures. Figure 9 shows data from Figure 7 graphed in an Arrhenius plot. The slope of the line fitting the points yields a reaction activation energy of -50 kJ/mol (-12 kcal/mol) for temperatures between 45 and 85 °C. Earlier studies of calcium oxidation by H₂O have also observed slower oxidation rates at higher temperatures and negative activation energies for calcium oxidation. One previous study measured an activation energy of -31.46 kJ/mol (-7.52 kcal/mol) between 20 and 70 °C.³ Other studies measured activation energies of -27.6 kJ/mol (-6.6 kcal/mol)² and -26.8 kJ/mol (-6.4 kcal/mol)¹ between 50 and 150 °C.

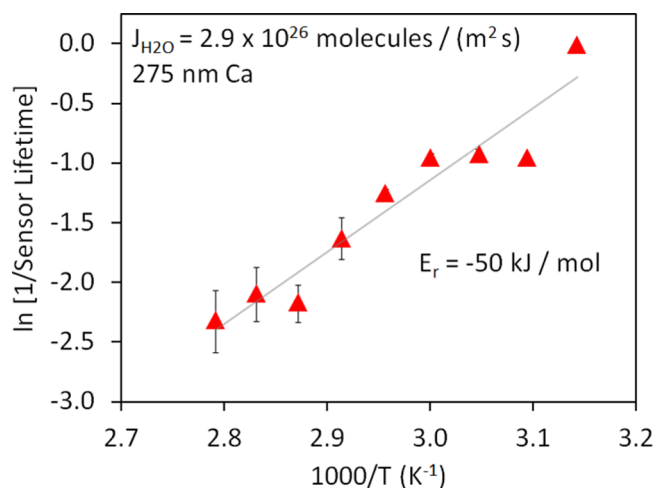


Figure 9. Arrhenius plot of the sensor lifetimes vs temperature in Figure 7. This Arrhenius plot yielded an activation energy of -50 kJ/mol for the reaction of H_2O with the Ca film.

F. H_2O Reaction Probability on Ca Film. The H_2O reaction probability, Γ_r , can be defined as the number of water molecules that react with the Ca film divided by the total number of water molecules impinging on the Ca film surface. This H_2O reaction probability, Γ_r , can be written as

$$\Gamma_r = N / (J_{\text{H}_2\text{O}} t_f) \quad (11)$$

where N is the total number of H_2O molecules that react with the Ca film. N can be determined from the mass gain occurring from time $t = 0$ to the sensor lifetime. $J_{\text{H}_2\text{O}}$ is the incident H_2O flux on the Ca film surface. The time required for the mass gain to reach a constant value is t_f , the sensor lifetime.

For all the experiments, the H_2O reaction probability averaged over the duration of the measurement was between $\Gamma_r = 1.2 \times 10^{-8}$ and 8.0×10^{-7} . This H_2O reaction probability is orders of magnitude smaller than unity. The H_2O reaction probability does change versus H_2O flux and temperature. For a fixed temperature, the H_2O reaction probability increases at higher H_2O fluxes as illustrated by Figure 6. For a fixed H_2O flux, the H_2O reaction probability decreases at higher temperatures as shown in Figure 7.

The H_2O reaction probability defined by eq 11 is averaged over the duration of the measurement. As shown in Figures 2–4, the calcium oxidation rate is not linear. Therefore, the H_2O reaction probability varies more than the estimated H_2O reaction probability based on the average over the entire experiment. The H_2O reaction probability is lower, compared with the average, in the lag region where there is little change in mass gain over time. The H_2O reaction probability in the lag region could be lower than the average by approximately a factor of 5. In addition, the H_2O reaction probability is higher than the average in the oxidation region where the oxidation rate rapidly increases. The H_2O reaction probability in the oxidation region could be higher than the average by approximately a factor of 2.

G. Experiments at Low H_2O Vapor Pressures. The measured H_2O reaction probabilities of $\sim 1 \times 10^{-8}$ are orders of magnitude lower than a H_2O reaction probability of unity. There is a chance that the low H_2O reaction probabilities result from the high water fluxes employed in these measurements. To measure H_2O reaction probabilities at much lower H_2O

fluxes, experiments were performed with Ca film thicknesses of 275 nm at H_2O pressures of 7×10^{-5} Torr at 30°C and 1×10^{-7} Torr at 50°C . These experiments required the use of a small high vacuum chamber that was positioned inside the temperature controlled oven of the ESPEC humidity chamber.

The Ca film was exposed to the H_2O pressure of 7×10^{-5} Torr at 30°C for 3.5 days. Over this time, the QCM showed that the Ca film remained in the lag region and the mass gain was only $2 \mu\text{g}/\text{cm}^2$. This mass gain in 3.5 days is consistent with a WVTR of 4.8×10^{-7} g/(m^2 day). This measured WVTR is much lower than the effective WVTR of 860 g/(m^2 day) based on the H_2O flux incident on the Ca film. This discrepancy argues for the noninstantaneous and nonlinear oxidation of calcium. The H_2O reaction probability, Γ_r , for this experiment was $\sim 5 \times 10^{-3}$. This H_2O reaction probability is greater than the H_2O reaction probabilities for higher H_2O fluxes.

A second experiment was performed at an H_2O pressure of 1×10^{-7} Torr at 50°C to explore the H_2O reaction probability at even lower H_2O fluxes. The base pressure in the small vacuum chamber was $\sim 1 \times 10^{-8}$ Torr. The Ca film was exposed to the H_2O pressure of 1×10^{-7} Torr for 20 days. The QCM measurements showed that the Ca film remained in the lag region and the mass gain for the Ca film was only $0.6 \mu\text{g}/\text{cm}^2$. The mass gain of $0.6 \mu\text{g}/\text{cm}^2$ over the time of 20 days is consistent with a WVTR of 3.4×10^{-8} g/(m^2 day). This measured WVTR is much lower than the effective WVTR of 1.2 g/(m^2 day) based on the H_2O flux incident on the Ca film. The H_2O reaction probability, Γ_r , for this experiment was $\sim 3 \times 10^{-3}$. This H_2O reaction probability is similar to the H_2O reaction probability derived from a H_2O pressure of 7×10^{-5} Torr.

IV. WVTR MEASUREMENTS WITH WATER VAPOR ACCUMULATION

Figure 10 shows the processes that occur in a standard Ca test measurement of the WVTR. The incoming H_2O flux, $\Phi_{\text{H}_2\text{O in}}$,

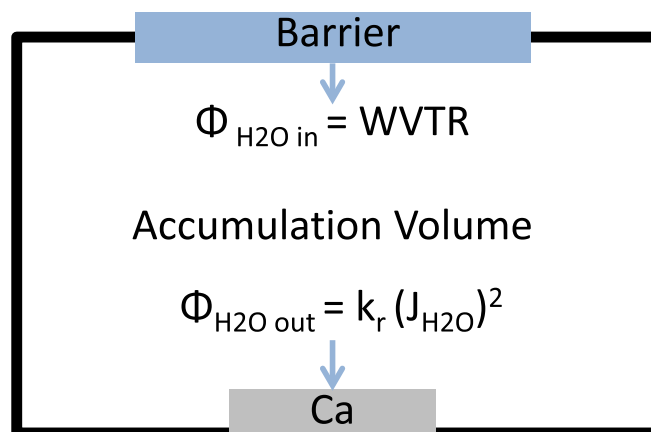


Figure 10. Schematic of processes that occur in the standard Ca test. Incoming H_2O flux enters the accumulation volume at given WVTR. Output H_2O flux leaves the accumulation volume at a rate of $k_r (J_{\text{H}_2\text{O}})^2$.

enters at a given WVTR. The H_2O then accumulates in the volume between the barrier and the Ca film. H_2O is also removed from the volume by the Ca film at the output H_2O flux, $\Phi_{\text{H}_2\text{O out}}$. The main difference between the standard Ca test and most of the experiments performed in this paper is that H_2O can accumulate in the volume between the barrier and the Ca film in the standard Ca test.

In the standard Ca test, H₂O that does not react with the Ca film during its first collision is still confined in the accumulation volume. The H₂O concentration in the accumulation volume will increase and the H₂O can collide repeatedly with the Ca film. In contrast, in most of the experiments performed in this paper, the H₂O pressure is fixed and a constant flux of H₂O impinges on the Ca film.

The output H₂O flux, $\Phi_{\text{H}_2\text{Oout}}$, is dependent on the H₂O reaction probability and the incident H₂O flux, $J_{\text{H}_2\text{O}}$, on the Ca film. Figure 10 expresses the output H₂O flux in terms of a rate constant, k_r , and $(J_{\text{H}_2\text{O}})^2$. The functional form, $\Phi_{\text{H}_2\text{Oout}} = k_r (J_{\text{H}_2\text{O}})^2$, is based on the second-order calcium oxidation kinetics observed in Figure 6. The rate constant, k_r , is obtained from an average over the sensor lifetime and is consistent with an H₂O reactive sticking coefficient much less than unity. If $\Phi_{\text{H}_2\text{Oout}} < \Phi_{\text{H}_2\text{Oin}}$, the H₂O pressure, $P_{\text{H}_2\text{O}}$, in the accumulation volume will increase until reaching the steady state conditions defined by $\Phi_{\text{H}_2\text{Oout}} = \Phi_{\text{H}_2\text{Oin}}$. The time required for the H₂O pressure to increase in the accumulation volume and approach the steady state conditions corresponds to the lag time.

A reliable WVTR measurement can be performed when $\Phi_{\text{H}_2\text{Oout}} = \Phi_{\text{H}_2\text{Oin}}$. To illustrate how reliable WVTR measurements are possible even when the Ca film oxidation kinetics are nonlinear, a mass balance equation with “Input = Output + Accumulation” was used to model the standard Ca test:

$$\text{WVTR} \times A_b = k_r (J_{\text{H}_2\text{O}})^2 A_{\text{Ca}} + \frac{V}{RT} \frac{dP}{dt} \quad (12)$$

In this equation, WVTR is the flux of H₂O into the apparatus volume through the barrier, A_b is the area of the barrier, V is the accumulation volume, P is the partial pressure of H₂O in the accumulation volume, k_r is the second-order reaction coefficient for H₂O at the surface of the Ca film, and A_{Ca} is the surface area of the calcium. In addition, t is time, T is temperature, and R is the gas constant.

Kinetic theory was used to calculate the flux of H₂O, $J_{\text{H}_2\text{O}}$, onto the surface of the Ca film surface as

$$J_{\text{H}_2\text{O}} = P / \sqrt{2\pi mkT} \quad (13)$$

where m is the mass of an H₂O molecule and k is the Boltzmann's constant. From the calcium oxidation measurements with no barrier shown in Figure 6, the reaction coefficients, k_r , were obtained for 30, 50, and 70 °C. Based on the fit to second-order calcium oxidation kinetics with the form $\Phi_{\text{H}_2\text{Oout}} = k_r (J_{\text{H}_2\text{O}})^2$, the reaction coefficients were $k_r = 4.73 \times 10^{-21} \text{ s}^{-1}$ at 30 °C, $k_r = 2.94 \times 10^{-21} \text{ s}^{-1}$ at 50 °C, and $k_r = 2.18 \times 10^{-21} \text{ s}^{-1}$ at 70 °C. These rate constants were derived from averages over the sensor lifetime and do not explicitly express the dependence of the Ca film oxidation kinetics on the extent of oxidation.

Integrating eq 12 with the boundary condition that $P[t=0] = 0$ results in the following expression:

$$P[t] = \sqrt{\frac{a}{b}} \tanh\left(\sqrt{ab} \frac{t}{c}\right) \quad (14)$$

where $a = \text{WVTR} \times A_b$, $b = A_{\text{Ca}} k_r / 2\pi mkT$, and $c = V/RT$. The flux of H₂O onto the surface of the Ca film, $J_{\text{H}_2\text{O}}$, can be determined by substituting the expression for $P[t]$ from eq 14 into eq 13. The total amount of H₂O reacted can be calculated by substituting $f = k_r (J_{\text{H}_2\text{O}})^2$ into eq 10. Figure 11 shows

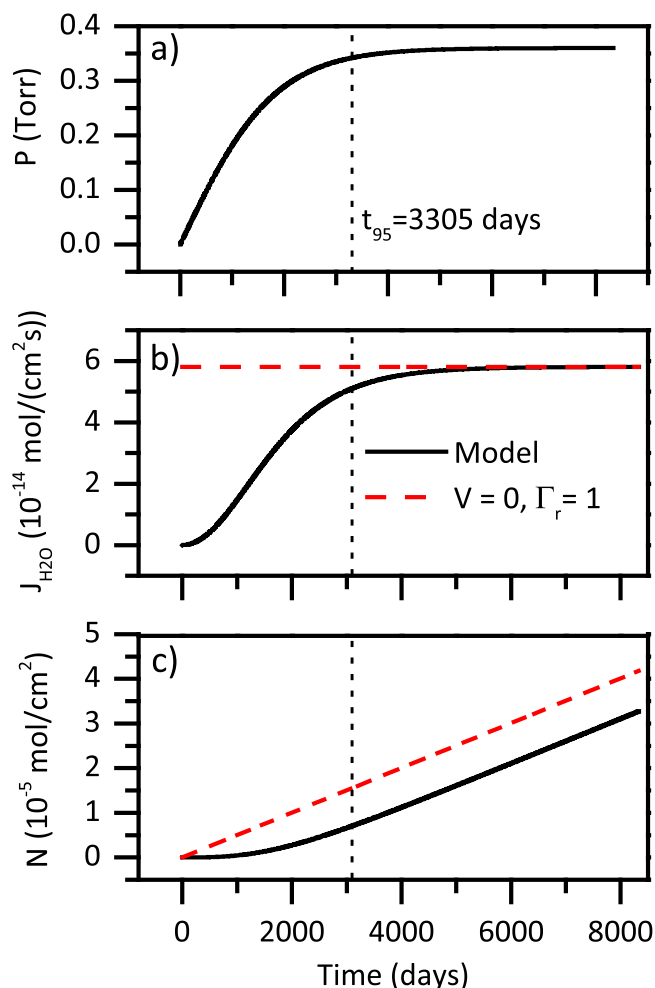


Figure 11. Modeling results for (a) H₂O pressure in accumulation volume, (b) H₂O flux, and (c) total number of H₂O molecules that react with Ca film using the experimental configuration shown in Figure 1a with WVTR = $1 \times 10^{-4} \text{ g}/(\text{m}^2 \text{ day})$, $V = 150 \text{ mL}$, $A_b = 2.85 \text{ cm}^2$, and $A_{\text{Ca}} = 0.316 \text{ cm}^2$. Dashed lines show results assuming an accumulation volume of $V = 0$ and an H₂O reaction probability of $\Gamma_r = 1$.

modeled profiles for the H₂O pressure (P), H₂O flux ($J_{\text{H}_2\text{O}}$), and total amount of H₂O reacted on the Ca film (N) for the experimental configuration in Figure 1a. The model assumed a gas diffusion barrier on a polymer with WVTR = $1 \times 10^{-4} \text{ g}/(\text{m}^2 \text{ day})$, an accumulation volume of $V = 150 \text{ mL}$, a polymer area of $A_b = 2.85 \text{ cm}^2$, and a Ca film area of $A_{\text{Ca}} = 0.316 \text{ cm}^2$.

The pressure in Figure 11a increases with time as the water transmission through the barrier slowly fills the accumulation volume. Based on the pressure in the accumulation volume, the H₂O flux onto the Ca film surface in Figure 11b also slowly increases with time. In contrast, the dashed line in Figure 11b shows the H₂O flux onto the Ca film surface assuming an accumulation volume of $V = 0$ and an H₂O reaction probability of $\Gamma_r = 1$. Figure 11c shows that the total amount of H₂O reacted on the Ca film is initially very low when the H₂O pressure and H₂O flux are low. The total amount of H₂O reacted on the Ca film grows linearly after reaching the steady state H₂O pressure.

The time to achieve the steady state pressure can be identified as an upper limit for the lag time. By setting $dP/dt = 0$ in eq 12, the steady state pressure is $P_{\text{ss}} = (a/b)^{1/2}$. By setting

$P[t]/P_{ss} = 0.95$, the time required for $P[t]$ to obtain 95% of the steady state pressure is

$$t_{95} = \frac{\sqrt{2\pi mk}}{R\sqrt{T}} \frac{V}{\sqrt{A_b \text{ WVTR} \times A_{Ca} k_r}} \tanh^{-1}(0.95) \quad (15)$$

The expression for t_{95} in eq 15 can be used to approximate the experimentally observed lag time in Ca test configurations assuming the Ca film is sufficiently thick.

Using the configuration shown in Figure 1a with $\text{WVTR} = 1 \times 10^{-4} \text{ g}/(\text{m}^2 \text{ day})$, an accumulation volume of $V = 150 \text{ mL}$, a polymer area of $A_b = 2.85 \text{ cm}^2$, and a Ca film area of $A_{Ca} = 0.316 \text{ cm}^2$, eq 15 at 30°C becomes

$$t_{95}[\text{days}] \cong \frac{33}{\sqrt{\text{WVTR} \left[\frac{\text{g}}{\text{m}^2 \cdot \text{day}} \right]}} \quad (16)$$

According to eq 16, the steady state pressure would be reached within 24 h only for gas diffusion barriers with $\text{WVTR} > 1092 \text{ g}/(\text{m}^2 \text{ day})$. For a barrier with a WVTR of $1 \times 10^{-4} \text{ g}/(\text{m}^2 \text{ day})$, 9 years (3305 days) would be required to reach steady state!

The predictions from eq 15 can be compared with the results in Figure 2. A lag time of $\sim 75 \text{ h}$ or $\sim 3 \text{ days}$ is observed in Figure 2 for the configuration shown in Figure 1a. In comparison, the predicted time to steady state conditions obtained from eq 15 is approximately $\sim 30 \text{ days}$ for a WVTR of $1.2 \text{ g}/(\text{m}^2 \text{ day})$. There is a discrepancy between the results and the prediction. This discrepancy arises from an insufficiently thick Ca film resulting in complete oxidation of the Ca film before reaching steady state conditions.

The time to reach the steady state pressure in the accumulation volume is a useful guide to determine the accuracy of various WVTR measurements of gas diffusion barriers on polymers using the Ca test. When an area of 1 cm^2 for both the polymer and Ca film is used, the accumulation volume can be determined based on the requirement that the steady state pressure is obtained in $\leq 24 \text{ h}$ with a WVTR of $1 \times 10^{-4} \text{ g}/(\text{m}^2 \text{ day})$ at 30°C . For these conditions, the required accumulation volume is $V \leq 0.05 \text{ cm}^3$. For a cylindrical accumulation volume with a cross-sectional area of 1 cm^2 , the required separation distance between the polymer and Ca film is $\leq 637 \mu\text{m}$. By decreasing the accumulation volume and increasing the polymer area and calcium area, the lag time required to obtain the steady state pressure will decrease for a given WVTR value. Smaller accumulation volumes enable faster measurements of accurate WVTR values.

Previous WVTR measurements using the Ca test have not recognized the importance of the small accumulation volumes required to achieve steady state pressures in short times and to obtain accurate WVTR values. However, many Ca test configurations do have small accumulation volumes and should achieve steady state in reasonable times. For the WVTR measurements performed with the Ca film deposited directly on the polymer,^{5,10,13,18,29,30} there is no accumulation volume and there should not be a problem with long lag times. However, these WVTR measurements may still observe the effects of nonlinear Ca film oxidation kinetics.

For the WVTR measurements where the polymer and Ca film are close but not intimately connected, the accuracy of the WVTR measurement will depend on the accumulation volume. Many of the previous WVTR measurements using this configuration have not reported the distance between the polymer

and the Ca film or the experimental configuration that defines the accumulation volume.^{7-9,31-35} The accuracy of these WVTR measurements will depend upon the accumulation volume. Other previous WVTR measurements have reported distances between the polymer and the Ca film that would produce accumulation volumes with extremely long lag times required to obtain steady state pressures.^{11,16}

In addition to using eq 15 to understand the proper steady state conditions for accurate Ca tests, this model can be used to determine WVTR values from existing Ca test data that was not obtained at steady state pressure. In Figure 12, the data from

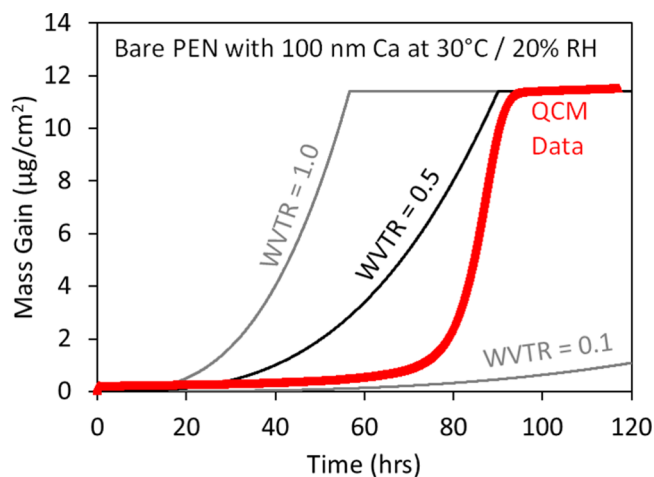


Figure 12. Mass gain vs time from Figure 2 for bare PEN polymer using test apparatus shown in Figure 1a compared with modeling results for WVTR s of 0.10, 0.50, and $1.00 \text{ g}/(\text{m}^2 \text{ day})$.

Figure 2 for the PEN polymer is displayed along with the model curves for WVTR values of 0.10, 0.50, and $1.00 \text{ g}/(\text{m}^2 \text{ day})$. The modeling suggests that the WVTR of the PEN polymer is $\sim 0.5 \text{ g}/(\text{m}^2 \text{ day})$. The modeled results for a $\text{WVTR} = 0.5 \text{ g}/(\text{m}^2 \text{ day})$ are not as nonlinear as the data because the model is based on a rate constant that is averaged over the sensor lifetime. This averaging loses the dependence of the Ca film oxidation kinetics on the extent of oxidation.

The WVTR of $\sim 0.5 \text{ g}/(\text{m}^2 \text{ day})$ for the $200 \mu\text{m}$ thick heat stabilized polyethylene-naphthalate (HSPEN) is close to the reported value of $1.2 \text{ g}/(\text{m}^2 \text{ day})$ for a $125 \mu\text{m}$ film of PEN.²⁴ The slight discrepancy is likely due to the thickness difference and may also result from different test conditions. The WVTR for PEN in this paper was measured at 30°C and 20% RH. The reported value for PEN was likely determined at higher relative humidities.

V. CONCLUSIONS

A new Ca test was developed based on quartz crystal microbalance (QCM) experiments to measure the oxidation of calcium films by water vapor. As the Ca film oxidized according to the reaction: $\text{Ca} + 2\text{H}_2\text{O} \rightarrow \text{Ca}(\text{OH})_2 + \text{H}_2$, the QCM measured the mass gain. The QCM measurements revealed a pronounced lag time prior to significant Ca film oxidation. This lag time was observed under a variety of experimental configurations and indicated that Ca film oxidation was not linear with H_2O flux.

Measurements of the times required for Ca film oxidation versus %RH at 30°C were not consistent with linear oxidation kinetics. Second-order kinetics in H_2O flux were obtained from

measurements of the Ca film oxidation times versus H₂O flux at 30, 50, and 70 °C. In addition, measurements of Ca film oxidation times versus temperature at constant H₂O flux were consistent with lower oxidation rates at higher temperatures and an activation barrier of -50 kJ/mol. These kinetics were consistent with a precursor-mediated desorption model.

Given the nonlinear Ca film oxidation kinetics, a model was developed to understand WVTR measurements using the Ca test. This modeling showed that the Ca test can yield reliable WVTR measurements under special circumstances. These circumstances occur when the accumulation volume between the polymer with a gas diffusion barrier and the Ca film is small enough to yield a short lag time. After this lag time, a steady state H₂O pressure can be established in the accumulation volume that yields an H₂O flux transmitted through the barrier that is equivalent to the H₂O flux removed by oxidation of the Ca film.

AUTHOR INFORMATION

Corresponding Author

*Tel.: 303-492-3398. E-mail: steven.george@colorado.edu.

Notes

The authors declare no competing financial interest.

ACKNOWLEDGMENTS

This work was supported by the Defense Advanced Research Projects Agency (DARPA) under Contract No. N10PC20168, a Phase II SBIR Grant to ALD NanoSolutions. M.J.Y. thanks the National Science Foundation (NSF) for an NSF Graduate Fellowship under Grant No. DGE 1144083. Any opinion, findings, and conclusions or recommendations expressed in this material are those of the authors and do not necessarily reflect the views of the NSF.

REFERENCES

- (1) Gregg, S. J.; Jepson, W. B. Oxidation of Calcium in Moist Oxygen. *J. Chem. Soc.* **1961**, 884–888.
- (2) Nissen, D. A. Low Temperature Oxidation of Calcium by Water Vapor. *Oxid. Met.* **1977**, *11*, 241–261.
- (3) Svec, H. J.; Apel, C. Metal-Water Reactions. 4. Kinetics of the Reaction between Calcium and Water Vapor. *J. Electrochem. Soc.* **1957**, *104*, 346–349.
- (4) Cros, S.; Firon, M.; Lenfant, S.; Trouslard, P.; Beck, L. Study of Thin Calcium Electrode Degradation by Ion Beam Analysis. *Nucl. Instrum. Meth. B* **2006**, *251*, 257–260.
- (5) Nisato, G.; Bouten, P. C. P.; Slikkerveer, P. J.; Bennett, W. D.; Graff, G. L.; Rutherford, N.; Wiese, L. Evaluating Higher Performance Diffusion Barriers: The Calcium Test. *Proc. Asia Display/IDW '01* **2001**, 1435–1438.
- (6) Lewis, J. S.; Weaver, M. S. Thin-Film Permeation-Barrier Technology for Flexible Organic Light-Emitting Devices. *IEEE J. Sel. Top. Quant. Elect.* **2004**, *10*, 45–57.
- (7) Garcia, P. F.; McLean, R. S.; Reilly, M. H.; Groner, M. D.; George, S. M. Ca Test of Al₂O₃ Gas Diffusion Barriers Grown by Atomic Layer Deposition on Polymers. *Appl. Phys. Lett.* **2006**, *89*, 031915.
- (8) Kim, T. W.; Yan, M.; Erlat, G.; McConnelee, P. A.; Pellow, M.; Deluca, J.; Feist, T. P.; Duggal, A. R.; Schaepekens, M. Transparent Hybrid Inorganic/Organic Barrier Coatings for Plastic Organic Light-Emitting Diode Substrates. *J. Vac. Sci. Technol. A* **2005**, *23*, 971–977.
- (9) Choi, J. H.; Kim, Y. M.; Park, Y. W.; Huh, J. W.; Ju, B. K.; Kim, I. S.; Hwang, H. N. Evaluation of Gas Permeation Barrier Properties Using Electrical Measurements of Calcium Degradation. *Rev. Sci. Instrum.* **2007**, *78*, 064701.
- (10) Paetzold, R.; Winnacker, A.; Henseler, D.; Cesari, V.; Heuser, K. Permeation Rate Measurements by Electrical Analysis of Calcium Corrosion. *Rev. Sci. Instrum.* **2003**, *74*, S147–S150.
- (11) Reese, M. O.; Dameron, A. A.; Kempe, M. D. Quantitative Calcium Resistivity Based Method for Accurate and Scalable Water Vapor Transmission Rate Measurement. *Rev. Sci. Instrum.* **2011**, *82*, 085101.
- (12) Chen, T. N.; Wu, D. S.; Wu, C. C.; Chiang, C. C.; Chen, Y. P.; Horng, R. H. High-Performance Transparent Barrier Films of SiO_x/SiN_x Stacks on Flexible Polymer Substrates. *J. Electrochem. Soc.* **2006**, *153*, F244–F248.
- (13) Kumar, R. S.; Auch, M.; Ou, E.; Ewald, G.; Jin, C. S. Low Moisture Permeation Measurement Through Polymer Substrates for Organic Light Emitting Devices. *Thin Solid Films* **2002**, *417*, 120–126.
- (14) Pilling, N. B.; Bedworth, R. E. The Oxidation of Metals at High Temperatures. *J. Inst. Met.* **1923**, *29*, 529–582.
- (15) Bertrand, J. A.; George, S. M. Evaluating Al₂O₃ Gas Diffusion Barriers Grown Directly on Ca Films Using Atomic Layer Deposition Techniques. *J. Vac. Sci. Technol. A* **2013**, *31*, 01A122.
- (16) Bertrand, J. A.; Higgs, D. J.; Young, M. J.; George, S. M. H₂O Vapor Transmission Rate through Polyethylene Naphthalate Polymer Using the Electrical Ca Test. *J. Phys. Chem. A* **2013**, *117*, 12026–12034.
- (17) Klumbies, H.; Muller-Meskamp, L.; Monch, T.; Schubert, S.; Leo, K. The Influence of Laterally Inhomogeneous Corrosion on Electrical and Optical Calcium Moisture Barrier Characterization. *Rev. Sci. Instrum.* **2013**, *84*, 024103.
- (18) Schubert, S.; Klumbies, H.; Muller-Meskamp, L.; Leo, K. Electrical Calcium Test for Moisture Barrier Evaluation for Organic Devices. *Rev. Sci. Instrum.* **2011**, *82*, 094101.
- (19) Cubicciotti, D. The Oxidation of Calcium at Elevated Temperatures. *J. Am. Chem. Soc.* **1952**, *74*, 557–558.
- (20) Gregg, S. J.; Jepson, W. B. The Oxidation of Calcium in Dry Oxygen. *J. Chem. Soc.* **1960**, 712–716.
- (21) Streiff, R. Study of Calcium Oxidation. Reaction Mechanisms. *Acta Metall.* **1968**, *16*, 1227–1238.
- (22) Bird, R.; Stewart, W.; Lightfoot, E. *Transport Phenomena*, 2nd ed.; John Wiley & Sons: New York, 2002.
- (23) Asmar, N. H. *Partial Differential Equations with Fourier Series and Boundary Value Problems*, 2nd ed.; Pearson Prentice Hall: Upper Saddle River, NJ, 2004.
- (24) Data on Teonex PEN from Teijin DuPont Films; http://www.tejindupontfilms.jp/english/product/pen_teo.html.
- (25) King, D. A.; Wells, M. G. Reaction Mechanism in Chemisorption Kinetics - Nitrogen on (100) Plane of Tungsten. *Proc. R. Soc. London, Ser. A* **1974**, *339*, 245–269.
- (26) Luntz, A. C.; Williams, M. D.; Bethune, D. S. The Sticking of O₂ on a Pt(111) Surface. *J. Chem. Phys.* **1988**, *89*, 4381–4396.
- (27) Coon, P. A.; Gupta, P.; Wise, M. L.; George, S. M. Adsorption and Desorption Kinetics for SiH₂Cl₂ on Si(111)7 × 7. *J. Vac. Sci. Technol. A* **1992**, *10*, 324–333.
- (28) Gupta, P.; Mak, C. H.; Coon, P. A.; George, S. M. Oxidation Kinetics of Si(111)7 × 7 in the Submonolayer Regime. *Phys. Rev. B* **1989**, *40*, 7739–7749.
- (29) Chen, T. N.; Wu, D. S.; Wu, C. C.; Chiang, C. C.; Chen, Y. P.; Horng, R. H. Improvements of Permeation Barrier Coatings Using Encapsulated Parylene Interlayers for Flexible Electronic Applications. *Plasma Process. Polym.* **2007**, *4*, 180–185.
- (30) Saitoh, K.; Kumar, R. S.; Chua, S.; Masuda, A.; Matsumura, H. Estimation of Moisture Barrier Ability of Thin SiN_x Single Layer on Polymer Substrates Prepared by Cat-CVD method. *Thin Solid Films* **2008**, *516*, 607–610.
- (31) Garcia, P. F.; McLean, R. S.; Groner, M. D.; Dameron, A. A.; George, S. M. Gas Diffusion Ultrabarrriers on Polymer Substrates Using Al₂O₃ Atomic Layer Deposition and SiN Plasma-Enhanced Chemical Vapor Deposition. *J. Appl. Phys.* **2009**, *106*, 023533.
- (32) Granstrom, J.; Villet, M.; Chatterjee, T.; Gerbec, J. A.; Jerkunica, E.; Roy, A. Multilayer Barrier Films Comprising Nitrogen Spacers

Between Free-Standing Barrier Layers. *Appl. Phys. Lett.* **2009**, *95*, 093306.

(33) Han, Y. C.; Jang, C.; Kim, K. J.; Choi, K. C.; Jung, K.; Bae, B. S. The Encapsulation of an Organic Light-Emitting Diode Using Organic-Inorganic Hybrid Materials and MgO. *Org. Elect.* **2011**, *12*, 609–613.

(34) Kim, E.; Han, Y.; Kim, W.; Choi, K. C.; Im, H. G.; Bae, B. S. Thin Film Encapsulation for Organic Light Emitting Diodes Using a Multi-Barrier Composed of MgO Prepared by Atomic Layer Deposition and Hybrid Materials. *Org. Elect.* **2013**, *14*, 1737–1743.

(35) Seo, S. W.; Jung, E.; Chae, H.; Cho, S. M. Optimization of Al₂O₃/ZrO₂ Nanolaminate Structure for Thin Film Encapsulation of OLEDs. *Org. Elect.* **2012**, *13*, 2436–2441.